Free Drying Shrinkage Performance of *Pinus sylvestris* L. Under Different Temperature and Humidity Conditions

Haojie Chai,* and Lu Li

Efficient utilization of wood is inseparable from high-quality drying, and analysis of its free shrinkage performance is essential to optimize the drying process. This study took *Pinus sylvestris* L. sawn timber (500 mm × 200 mm × 50 mm) as the research object and adopted the image analysis method to analyze the influence rules of different temperatures and axial positions of the test material on the free dry shrinkage coefficient of each layer of specimens in the thickness direction. The free shrinkage coefficients of each layer in the thickness direction of the test material decreased from the maximum value of the first layer near the tangential direction (0.282%, 0.275%, 0.267%, at 60 °C, 80 °C, and 100 °C, respectively) to the minimum value of the ninth layer near the radial direction (0.248%, 0.249%, 0.227%); except for the near-radial layers, when temperature increased from 60 °C to 100 °C the free shrinkage coefficients of other representative layers decreased with increased temperature. The first layer's free shrinkage coefficient decreased from 0.282% to 0.267%, and the fifth layer decreased from 0.264% to 0.243%. The difference of free shrinkage coefficients between corresponding layers at different axial positions of the test material was less than 0.017%, and the size stability of the corresponding layers at axial positions was high.

DOI: 10.15376/biores.19.3.6444-6458

Keywords: Temperature and humidity pretreatment; Free shrinkage performance; Drying quality; Image analysis method

*Contact information: School of Artificial Intelligence, Henan Institute of Science and Technology, Xinxiang, 453003, China; School of Fine Arts and Design, Henan Institute of Science and Technology, Xinxiang, 453003, China; *Corresponding author: nefuchj@163.com*

INTRODUCTION

The asynchronous shrinkage caused by uneven distribution of moisture content and anisotropic shrinkage of sawn timber during drying is the main reason for the generation of drying stress and drying defects. Research on the variation law of drying strain during drying process is of great significance for further exploring drying stress, optimizing the drying process, improving drying quality, and reducing drying time. Free shrinkage of wood is a phenomenon in which thin and small test pieces undergo a change in size due to the loss of water in the cell walls during slow drying (desorption), while the drying stress generated can be ignored (Gao and Wang 2022). Temperature is an important factor affecting the free shrinkage of wood. Exploring the influence of temperature and axial position of test materials on the free shrinkage performance of each layer of test pieces in the thickness direction under corresponding temperature and humidity conditions is of great significance for further studying the anisotropic shrinkage of wood.

Recent research in China and abroad on the free shrinkage performance of wood mainly includes the following: Tu (2004, 2009) explored the free shrinkage and rheological laws of Masson's pine, as well as the drying stress model; Zhan *et al.* (2002, 2009) studied the free shrinkage deformation of *Larix gmelinii* and *Tsuga heterophylla* at different temperatures; Quan and Pang (2012) studied the tangential shrinkage coefficient of irregular shaped *Larix gmelinii* small logs, and identified two trends of shrinkage coefficient along the radial direction at the same temperature. Zhao *et al.* (2015) summarized the research status of the establishment and solution of heat and mass transfer models during the drying process in China and elsewhere based on water migration, energy transfer, stress-strain and numerical solution methods, and proposed that the multidimensional heat and mass transfer that conforms to the actual drying conditions. Based on such findings, coupled mathematical model of heat and mass-stress strain considering the wood shrinkage phenomenon can be expected to be the focus of research in the future. Yang *et al.* (2018) and Zhang *et al.* (2018) studied the free shrinkage law of *Eucalyptus urophylla grandis* under different thickness conditions; Almeida *et al.* (2007), Perre and Huber (2007) and Perre *et al.* (2016) studied the free shrinkage of wood at the cellular level. Foreign scholars have rich research results on the free shrinkage characteristics of wood, but there are still the following problems: (1) Regarding the reference size for calculating the mechanical adsorption creep strain when the free shrinkage reaches the target moisture content, it is obtained by drying the strain test piece to the target moisture content after eliminating plastic deformation by steaming. It is doubtful and needs to be verified whether the steaming method can completely restore the plastic deformation. (2) Regarding the research on free shrinkage performance, small test pieces have been used to calculate only the shrinkage rates in the tangential, radial, and fiber directions at a certain moisture content below the fiber saturation point and when completely dry, and the shrinkage coefficients in the three directions are calculated accordingly. Because the standard test pieces used are inevitably subject to stress under faster drying conditions, it is difficult to ensure that the above-mentioned shrinkage is free shrinkage.

Based on this, this study took 50-mm-thick *Pinus sylvestris* L. sawn timber as the object, balanced the free shrinkage performance test specimens under different temperature and humidity conditions, measured the free shrinkage performance parameters of each specimen at different temperatures, and used their mean values to represent the free shrinkage performance of each specimen in the thickness direction of the test material. The study also analyzed the influence of temperature and the axial position of the test material on the free shrinkage coefficients of each layer of specimens in the thickness direction.

EXPERIMENTAL

Materials

As shown in Fig. 1, 50-year-old *Pinus sylvestris* L. from the Daxing'anling forest region was processed into a tangential board sawn timber with dimensions of 4000 mm (length, fiber direction) × 200 mm (width, upper surface layer near the tangential direction, lower surface layer near the radial direction) × 50 mm (thickness, slightly radial direction), with an initial moisture content ranging from 68.5% to 80.8%. Each time, 12 test pieces (500 mm×200 mm×50 mm) were used for the drying experiment. Four pieces of conventional drying test materials with a length of 500 mm were cut from each sawn timber (used for the detection of actual shrinkage performance during the conventional drying process) as well as free shrinkage performance test pieces from both ends of each sawn timber (without obvious defects, six pieces each). The test pieces measured 10 mm (fiber direction) × 200 mm × 50 mm and were then decomposed into nine layers along the thickness of the sawn timber to obtain free shrinkage performance test specimens for each layer in the thickness direction of the test material (numbered in order from the upper surface layer near the tangential direction to the lower surface layer near the radial direction).

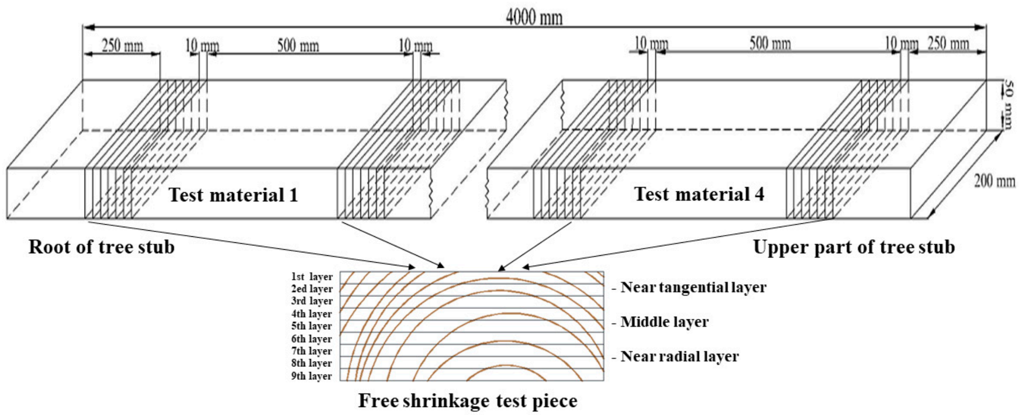

Fig. 1. Preparation of experimental specimen (Creative Commons Attribution (CC BY) license Zhu *et al.* 2021)

Experimental Method

Application of image analysis method

The vernier caliper is commonly used to measure the dimensions of test materials during the drying process. However, due to a considerable number of manual errors and relatively low precision, there are many limitations and defects in its application. Digital image analysis is currently a commonly used method for accurately measuring object dimensions. Through obtaining images of objects with scales using high-resolution cameras (EOS R100 Canon), specific dimensions of the objects can be derived through analysis and processing of the relevant images using ImageJ software (an open-source image processing software developed based on Java). This method has the advantages of efficient, non-contact measurement, high precision, and low human error. In this article, the relevant data were obtained using image analysis. First, the images were collected, then the point distances were measured, and finally the calculations of each strain were carried out through digital image processing.

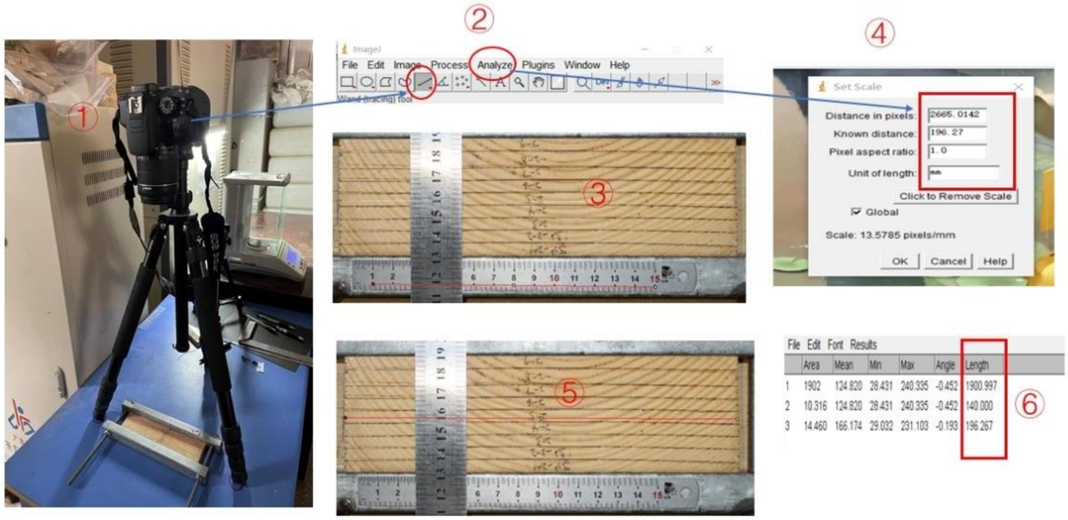

Fig. 2. Flow chart of image parsing operation

The operation process of the image analysis method is shown in Fig. 2. Because the test material holder in the experiment has a certain depth, attention should be paid to the impact of the depth of field difference on the true value of the test material size during photography, and the test material and the scale should be kept on the same horizontal plane as much as possible. At the same time, to improve the reliability of the data, the placement position of the fixture for each photograph should be kept consistent.

Measurement of free drying shrinkage performance

The free shrinkage of wood is shrinkage that is not subject to internal and external stress. To ensure that the free shrinkage performance test specimens are not subject to stress during the drying process, they are processed into thin and small test specimens with dimensions of 10 mm (fiber direction) × 200 mm × 5.5 mm as shown in Fig. 1. After that, a DHS-225 constant temperature and humidity drying chamber （temperature range 0 °C to 150 °C ±0.5 °C, humidity range 35% to 98% RH±2%, Beijing Yashilin Laboratory Equipment Co., Ltd.）was used to slowly dry them under the temperature and humidity conditions shown in Table 1 (Zhu *et al.* 2021). Whenever the specimens are dried to the desorption equilibrium moisture content (slightly higher than the corresponding equilibrium moisture content listed in the table) under each temperature and humidity condition, the weight and length of each test strip were measured, and the moisture content and free shrinkage rate of the test specimen at that time were calculated using Eqs. 1 and 2, respectively. After the last weight and size measurement at the same temperature (at the lowest equilibrium moisture content), the specimens were baked to absolute dryness at a temperature of 103 ± 2 ℃, and the absolute dry weight was measured. To study the effect of temperature on free shrinkage performance, the dry bulb temperatures were set to 60, 80, and 100 ℃.

The formula for calculating the moisture content of *Pinus sylvestris* test materials and specimens is as shown in Eq. 1 (Zhu *et al.* 2021),

$$MC_t = \frac{G_t - G_d}{G_d} \times 100\% \tag{1}$$

where MC_t is the moisture content of the test material or specimen at time t (%), G_t is the weight of the test material or specimen at time t (g), and G_d is the absolute dry weight of the test material or specimen (g).

The free shrinkage rate of the specimen is calculated according to Eq. 2,

$$y_{mc} = \frac{L_0 - L_{mc}}{L_0} \times 100\% \tag{2}$$

where y_{mc} is the shrinkage rate of the specimen at moisture content MC (%), L_0 is the initial length of the specimen (mm), and L_{mc} is the length of the specimen at moisture content MC (mm).

The free shrinkage coefficient is the ratio of the change in free shrinkage rate below the fiber saturation point to the corresponding change in moisture content. Its calculation formula is as shown in Eq. 3,

$$K = \frac{y_{mc}}{FSP - MC} \tag{3}$$

where K is the free shrinkage coefficient of the specimen (%), MC is the moisture content of the specimen at a certain time below the fiber saturation point (%), y_{mc} is the free shrinkage rate of the specimen at moisture content MC (%), and FSP is the fiber saturation point of the specimen in the corresponding layer (%).

The free shrinkage coefficient of the specimen is the slope of the relationship curve between the free shrinkage rate and moisture content obtained from the experiment, which is determined by the slope of the fitting curve equation of the curve.

Table 1. Drying Conditions of Free Drying Shrinkage Test Specimen

Dry-bulb Temperature (°C)	Wet-bulb Temperature (°C)	Relative Humidity (%)	Equilibrium Moisture Content (%)
60	60	100	27
	59	95	21
	57	86	15.5
	53	69	10.5
	47	49	7
	43	30	4.5
80	60	100	25
	59	96	19
	57	88	14.5
	53	73	10
	47	55	7
	43	39	5
100	60	100	22
	59	97	16.5
	57	90	13
	53	77	9.5
	47	61	6.5
	43	45	4.5

RESULTS AND DISCUSSION

Drying Rate Analysis

Figure 3 shows the drying treatment curves of the test materials under three temperature conditions. The average initial moisture contents of the specimens corresponding to 60, 80, and 100 ℃ are 68.5%, 77.1%, and 80.8%, respectively, with the maximum initial layered moisture content gradients of 28.1, 28.2, and 24.9%/cm, respectively. The equilibrium times under the three temperature conditions were 68 h, 64 h, and 60 h, respectively, and the specimen equilibrium rates range from 0.95 to 1.19%/h. As shown in Fig. 3, a higher temperature resulted in a faster decrease in the moisture content, and a steeper specimen equilibrium curve. The maximum equilibrium treatment rate was 1.19%/h at 100 ℃.

Figure 3 shows that at the initial stage of equilibrium treatment, the moisture content of the three groups of specimens rapidly decreased, and the weight of the specimens basically remained unchanged at around 20 h; they reached an equilibrium state under the temperature and humidity conditions set by the constant temperature and humidity chamber. As the humidity decreased, the rate at which the specimens reached the moisture sorption-desorption equilibrium accelerated. Because the criterion for judging the equilibrium state is that the moisture content of the specimen remains stable during two consecutive measurements, the three curves show a step-like decreasing trend in the middle and later stages of the experiment. Equilibrium treatment can accurately determine the size changes of the specimens corresponding to different moisture contents, thereby improving the accuracy and reliability of the free shrinkage dimensions of the specimens under the corresponding moisture contents.

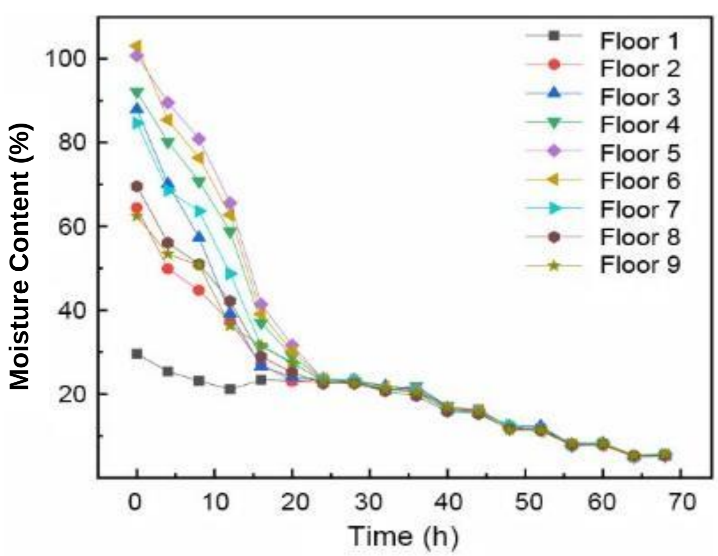

(a) Treatment temperature 60 °C

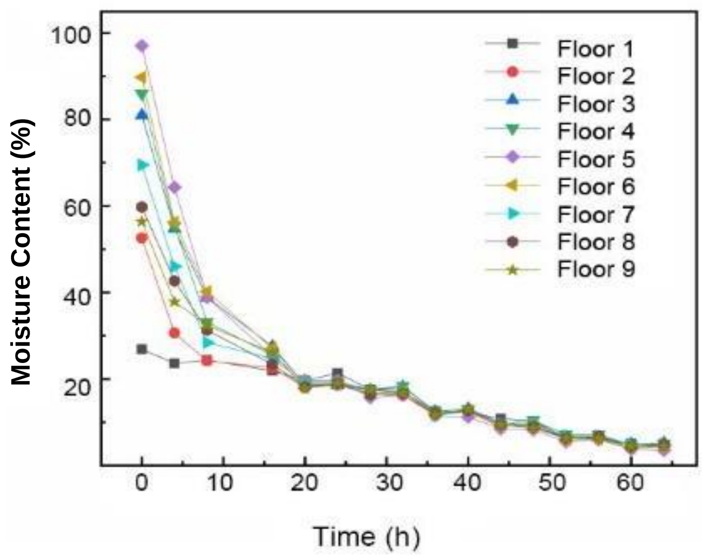

(b) Treatment temperature 80 °C

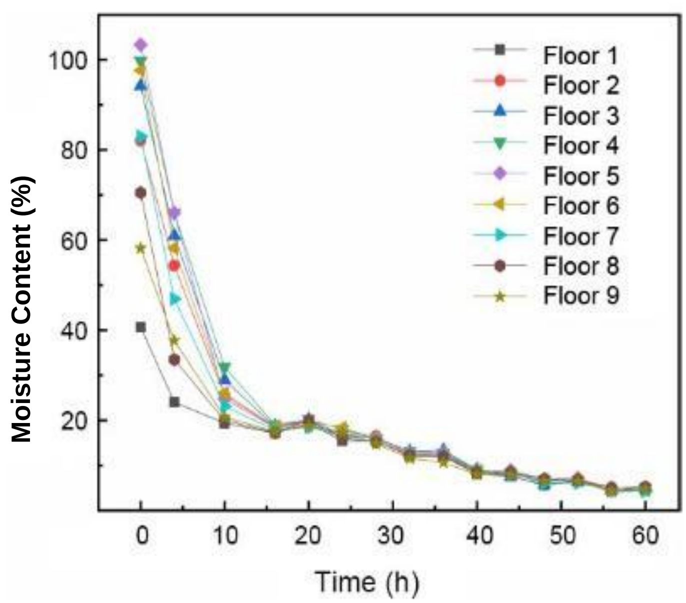

(c) Treatment temperature 100 °C

Fig. 3. Moisture content *vs.* time at 60, 80, and 100 °C

Free Drying Shrinkage Coefficient of Each Layer Along the Thickness Direction of the Test Material

Tables 2, 3, and 4 present the fitting equation parameters for the free shrinkage laws of different layers of *Pinus sylvestris* at different temperatures.

Table 2. Fitting Equation Parameters of Free Drying Shrinkage Law of Sawn Timber with Different Layer Widths at 60 °C

Level Number	*K* (%)	*K* Deviation	Y_{max} (%)	y_{max} Deviation	FSP (%)	FSP Deviation	Determination Coefficient (R^2)
layer 1	0.282	0.0049	6.88	0.044	24.38	0.42	0.9965
layer 2	0.281	0.0070	6.96	0.128	24.78	0.33	0.9988
layer 3	0.278	0.0082	6.97	0.145	25.11	0.42	0.9987
layer 4	0.275	0.0053	6.87	0.129	24.97	0.33	0.9979
layer 5	0.264	0.0044	6.73	0.099	25.49	0.52	0.9980
layer 6	0.258	0.0049	6.47	0.189	25.07	0.49	0.9955
layer 7	0.262	0.0092	6.53	0.228	24.93	0.77	0.9959
layer 8	0.258	0.0077	6.30	0.197	24.37	0.54	0.9968
layer 9	0.247	0.0068	6.13	0.096	24.81	0.69	0.9982

Note: The symbols *K*, y_{max}, and FSP in the table represent the free drying shrinkage coefficient, full drying free drying shrinkage rate, and fiber saturation point of the specimen in the experiment, respectively.

Table 3. Fitting Equation Parameters of Free Drying Shrinkage Law of Sawn Timber with Different Layer Widths at 80 °C

Level Number	*K* (%)	*K* Deviation	Y_{max} (%)	y_{max} Deviation	FSP (%)	FSP Deviation	Determination Coefficient (R^2)
layer 1	0.275	0.0083	6.69	0.157	24.33	0.54	0.9966
layer 2	0.273	0.0050	6.91	0.112	24.78	0.52	0.9980
layer 3	0.275	0.0063	6.89	0.126	25.04	0.27	0.9968
layer 4	0.273	0.0049	6.89	0.077	25.22	0.32	0.9983
layer 5	0.261	0.0034	6.54	0.114	25.09	0.27	0.9941
layer 6	0.259	0.0043	6.50	0.0733	25.08	0.32	0.9997
layer 7	0.266	0.0057	6.52	0.133	24.54	0.23	0.9905
layer 8	0.258	0.0084	6.31	0.115	24.43	0.58	0.9979
layer 9	0.249	0.0046	6.06	0.156	24.33	0.85	0.9976

Note: The symbols *K*, y_{max}, and FSP in the table represent the free drying shrinkage coefficient, full drying free drying shrinkage rate, and fiber saturation point of the specimen in the experiment, respectively.

Table 4. Fitting Equation Parameters of Free Drying Shrinkage Law of Sawn Timber with Different Layer Widths at 100 °C

Level Number	*K* (%)	*K* Deviation	Y_{max} (%)	y_{max} Deviation	FSP (%)	FSP Deviation	Determination Coefficient (R^2)
layer 1	0.267	0.0026	6.80	0.099	25.41	0.27	0.9989
layer 2	0.263	0.0041	6.73	0.081	25.60	0.26	0.9981
layer 3	0.264	0.0037	6.89	0.103	26.12	0.33	0.9981
layer 4	0.262	0.0046	6.73	0.131	25.71	0.57	0.9977
layer 5	0.243	0.0058	6.42	0.132	26.38	0.32	0.9878
layer 6	0.232	0.0039	6.10	0.081	26.25	0.27	0.9979
layer 7	0.234	0.0041	6.05	0.125	25.77	0.33	0.9963
layer 8	0.229	0.0100	5.83	0.147	25.47	0.64	0.9934
layer 9	0.227	0.0046	5.70	0.133	25.15	0.75	0.9965

Note: The symbols *K*, y_{max}, and FSP in the table represent the free drying shrinkage coefficient, full drying free drying shrinkage rate, and fiber saturation point of the specimen in the experiment, respectively.

It can be seen that the minimum value of the determination coefficient of the fitting equation was 0.9878, which is close to 1 and indicates a high correlation. This suggests that using the equation to describe the corresponding free shrinkage performance has a high degree of accuracy and reliability. The deviations in the fitted free shrinkage coefficient and the total drying free shrinkage rate are small, indicating that there are small differences in the free shrinkage performance of the corresponding layers on the thickness of adjacent test pieces at both ends of the test material, as well as small measurement errors. Therefore, using the mean values of these two parameters in the table to characterize the free shrinkage performance of the corresponding layer of the test material has a high degree of accuracy.

The Free Drying Shrinkage Difference of Each Layer Along the Thickness Direction of the Test Material

Figure 4 illustrates the shrinkage coefficients and total free drying shrinkage rates of various layers along the thickness direction of the test material at different temperatures. The results indicate that the first layer had the highest free shrinkage coefficient (above 0.267%) and total free drying shrinkage rate (above 6.69%), with decreasing values in the subsequent layers. This is mainly attributed to the anisotropy of shrinkage caused by the arrangement angle of cell wall fibrils. Because the first layer is close to the tangential direction and the ninth layer is close to the radial direction, the tangential shrinkage coefficient is approximately twice that of the radial coefficient, leading to the observed results. The differences in shrinkage coefficients between the first and ninth layers at 60, 80, and 100 ℃ were 0.035%, 0.026%, and 0.041%, respectively. It can be seen that the anisotropy of shrinkage among different layers of *Pinus sylvestris* L. test material was the greatest at 100 ℃, while the other two temperatures had less influence on the anisotropy of shrinkage and no regular pattern is observed.

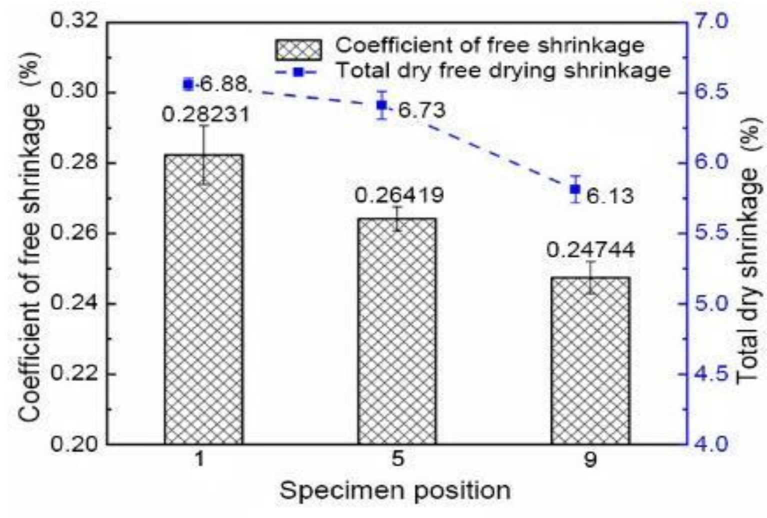

(a) At 60 °C

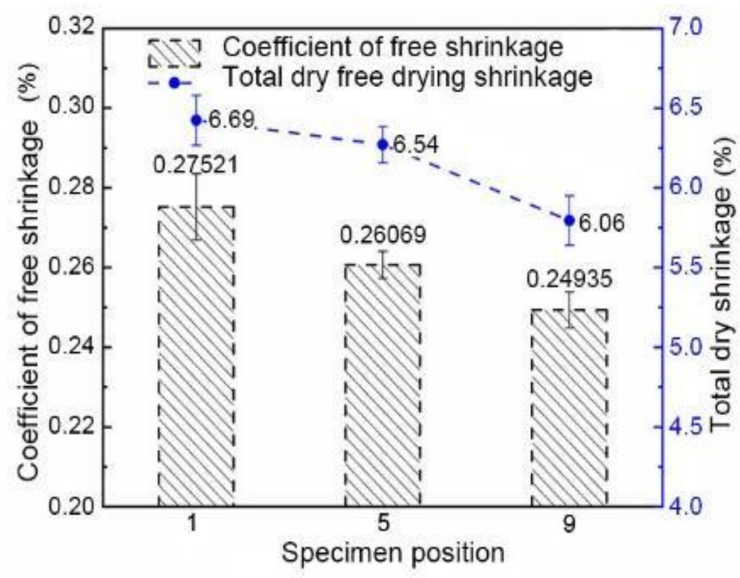

(b) At 80 °C

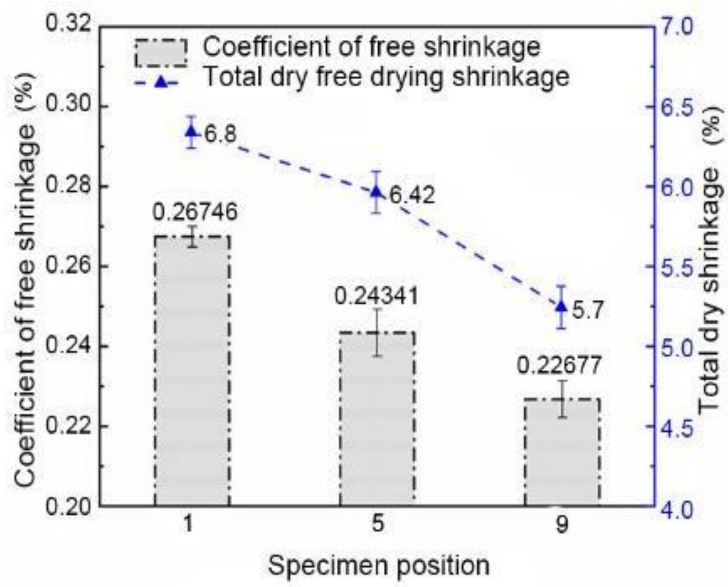

(c) At 100 °C

Fig. 4. Coefficient of free shrinkage *vs.* sample position at 60, 80, and 100 °C

Effect of Axial Position of Test Material on Free Drying Shrinkage

Table 5 presents the mean values and deviations of the free shrinkage coefficients in the width direction of the representative layers on the thickness of adjacent test specimens at both ends of the four different sections of the *Pinus sylvestris* L. in the length direction shown in Fig. 1. At 60 ℃, the largest difference in free shrinkage coefficient occurs in the 9th layer between specimen 3 and specimen 4, with a difference of 0.017% (followed by a difference of 0.016% in the 5th layer between specimen 2 and specimen 3 at 100 ℃). Under this temperature condition, the difference in the free shrinkage coefficient of the 1st layer in the axial direction of the specimen was within 0.009%. This indicates that there is a small difference in the free shrinkage coefficient in the width direction of the representative layer on the thickness of *Pinus sylvestris* L. at different axial positions under the same temperature conditions. It is speculated that the straight texture of *Pinus sylvestris* L. results in similar free shrinkage properties at different axial positions.

Table 5. Free Drying Shrinkage Coefficient of Sawn Timber in Different Parts of the Length Direction

Temp (°C)	Level Number	Test Material 1 *K* (%)	Deviation	Test Material 2 *K* (%)	Deviation	Test Material 3 *K* (%)	Deviation	Test Material 4 *K* (%)	Deviation
60	layer 1	0.282	0.0049	0.280	0.0042	0.278	0.0021	0.287	0.0069
	layer 5	0.264	0.0044	0.266	0.0053	0.255	0.0029	0.269	0.0060
	layer 9	0.247	0.0068	0.243	0.0046	0.239	0.0068	0.258	0.0041
80	layer 1	0.275	0.0083	0.275	0.0057	0.283	0.0012	0.277	0.0050
	layer 5	0.261	0.0034	0.260	0.0025	0.257	0.0046	0.266	0.0062
	layer 9	0.249	0.0046	0.241	0.0045	0.250	0.0076	0.250	0.0102
100	layer 1	0.267	0.0024	0.266	0.0060	0.267	0.0020	0.272	0.0109
	layer 5	0.244	0.0058	0.247	0.0056	0.231	0.0107	0.242	0.0075
	layer 9	0.227	0.0047	0.235	0.0077	0.227	0.0109	0.223	0.0034

Note: Test specimen 1 is near the root of the tree, and test specimen 4 is near the crown of the tree

Influence of Temperature on the Free Drying Shrinkage Performance of Each Layer in the Thickness Direction of the Test Material

Figure 5 illustrates the relationship between the free shrinkage coefficient of each layer of the test specimens along the thickness direction and temperature. It can be observed that except for the 9th layer, the free shrinkage coefficient in the width direction of the other layers decreased as the temperature rose. However, the 9th layer experienced a slight increase in the free shrinkage coefficient as the temperature rose from 60 to 80 °C, followed by a decrease with further temperature increase. The differences in the free shrinkage coefficients of the representative layers (the 1st, 5th, and 9th layers) in the thickness direction of the test material at 60 and 100 °C were 0.015%, 0.021%, and 0.022%, respectively. This indicates that the influence of temperature on the free shrinkage coefficient of the layers close to the tangential direction is less than that on the layers close to the radial direction in *Pinus sylvestris*. The factors that affect the free shrinkage coefficient of *Pinus sylvestris* L. under different temperatures are not yet clear.

Figure 4 represents the fiber saturation points of different layers of test specimens obtained by extrapolation at different temperatures. As the temperature rose, the fiber saturation point slightly decreased and then increased. It is speculated that the increase in temperature enhances the activity of cellulose molecular chains in the cell wall, leading to the accumulation of cellulose molecular chains at higher moisture contents (due to the disappearance of hydrogen bonds and the expulsion of water molecules from the non-crystalline regions of cellulose). This results in a deviation between the relationship between the fiber saturation point and temperature and the theoretical situation (Ping *et al.* 2018).

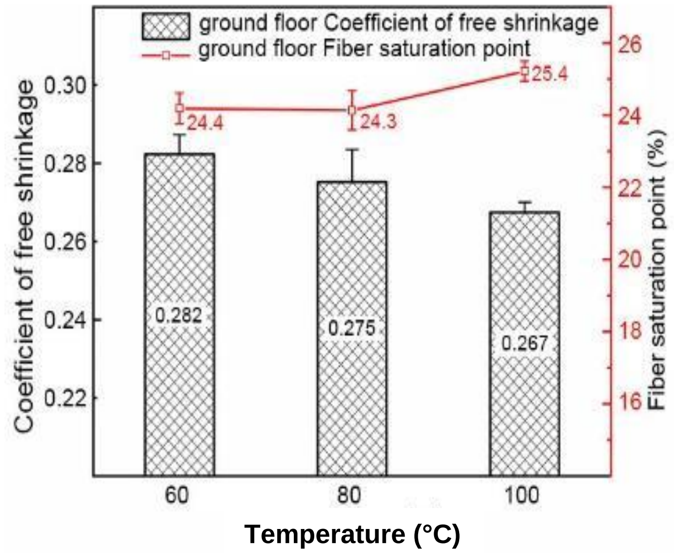

(a) Layer 1

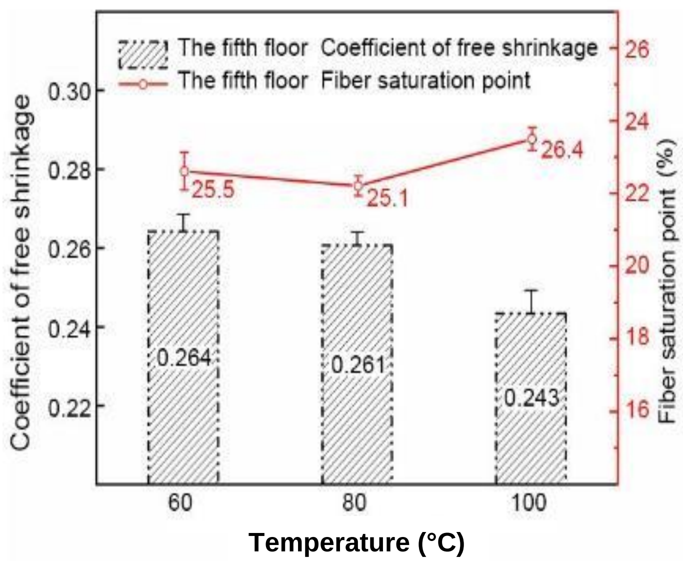

(b) Layer 5

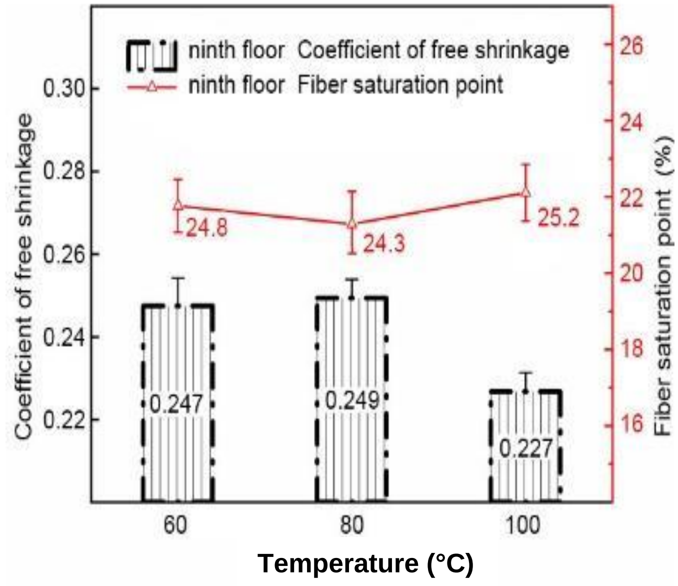

(c) Layer 9

Fig. 5. Effect of temperature on the free shrinkage coefficient of specimens in each layer along the thickness direction of the test material

CONCLUSIONS

1. This study offers an accurate detection method for the free shrinkage performance of each layer specimen along the thickness direction of wood. This approach can provide a reference for the detection of free shrinkage performance in other directions.
2. The free shrinkage coefficient of each layer of the test piece along the thickness direction of the test material showed a decreasing trend from the maximum value of the first layer near the chord direction to the minimum value of the ninth layer near the radial direction.
3. When the temperature rose from 60 to 100 ℃, except for the layer close to the radial direction, the free shrinkage coefficient of other representative layers decreased with increasing temperature.
4. The difference in free shrinkage coefficient between corresponding layers at different axial positions of the test material was less than 0.017%, indicating high dimensional stability of the corresponding layers at its axial positions.
5. For the next research direction, it will be important to ensure the accuracy of the free shrinkage coefficient of wood, consider the influence of temperature on the free shrinkage performance of wood, and establish the functional relationship between temperature and the free shrinkage of wood.

ACKNOWLEDGMENTS

This work was financially supported by Key research Project of higher education institutions in Henan Province (23A520034).

REFERENCES CITED

Almeida, G., Gagné, S., and Hernández, R.-E. (2007). "An NMR study of water distribution in hardwoods at several equilibrium moisture contents," *Wood Science and Technology* 41(4), 293-307. DOI: 10.1007/s00226-006-0116-3

Gao, J. M., and Wang, X. M. (2022). *Wood Drying Science*, Science Press, Beijing.

Perré, P., and Huber, F. (2007). "Measurement of free shrinkage at the tissue level using an optical microscope with an immersion objective: Results obtained for Douglas fir (*Pseudotsuga menziesii*) and spruce (*Picea abies*)," *Annals of Forest Science* 64(3), 255-265. DOI: 10.1051/forest:2007003

Perré, P., Almeida, G., Ayouz, M., and Frank, X. (2016). "New modelling approaches to predict wood properties from its cellular structure: Image-based representation and meshless methods," *Annals of Forest Science* 73(1), 147-162. DOI: 10.1007/s13595-015-0519-0

Ping, L. J., Wang, X. M., Yan. Y., Chen, Y.L. (2018). "Study on unsteady-state moisture transfer and energy consumption in high temperature drying process of *Pinus sylvestris* var. *Mongolica* Litv.," *Forest Products Industry* 45(9), 28-32,51. DOI: 10.19531/j.issn1001-5299.201809007

Quan, S. H., and Pang, F.Y. (2012). "Effect of temperature on tangential shrinkage coefficient of small-diameter larch profiles," *Forest Engineering* 28(06), 11-14. DOI: 10.3969/j.issn.1001-005X.2012.06.004

Tu, D. Y., Gu, L. B., Du, G. X., and Liu, B. (2004). "Study on the drying strain of *Pinus massoniana* planks during drying process," *Journal of Nanjing Forestry University (Natural Science Edition)* 2004(04), 23-28.

Tu, D. Y., and Liu, B. (2009). "Research on the stress model of wood drying," *Journal of Nanjing Forestry University (Natural Science Edition)* 33(03), 87-91.

Yang, L., Fu, Q. Y., Liu, H. H., and Wu, Z. H. (2018). "Determination of free shrinkage rate and fiber saturation point of *Eucalyptus urophylla* x *E. grandis*," *Journal of Northeast Forestry University* 46(04), 39-42. DOI: CNKI:SUN:DBLY.0.2018-04-008

Zhan, J. F., Gu, J. Y., and Cai, Y. C. (2009). "Dynamic viscoelastic properties of Larch plank during conventional drying process," *Journal of Beijing Forestry University* 31(01), 125-129. DOI: 10.3321/j.issn:1000-1522.2009.01.021

Zhan, J. F., Ai, M. Y., and Gu, J. Y. (2002). "Characteristics, comparison and analysis of various control methods for conventional drying of wood," *Forestry Machinery & Woodworking Equipment* 30(01), 4-6. DOI: 10.3969/j.issn.2095-2953.2002.01.001

Zhang, C. J., Zhang, Y. T., Xu, S. N., Su, S., Liu, H. H., Yang, L., and Huang, Q. T. (2018). "Determination of free shrinkage rate of *Eucalyptus urophylla* x *E. grandis* based on scanning image method," *Furniture* 39(06), 31-34.

Zhao, J. Y., Cai, Y. C., and Fu, Z. Y. (2015). "Research status of mathematical model of heat and mass transfer in wood drying process," *Journal of Beijing Forestry University* 37(07), 123-128. DOI: 10.13332/j.1000--1522.20140471

Zhu, X. D., Zhao, J. Y., Gao, W. H., Qian, C., Duan, Y. J., Niu, S. C., and Cai, Y. C. (2021). "Laws governing free and actual drying shrinkage of 50 mm thick Mongolian Scotch pine timber," *Forests* 12(11), 1500. DOI: 10.3390/f12111500

Article submitted: April 10, 2024; Peer review completed: July 1, 2024; Revised version received: July 15, 2024; Accepted: July 16, 2024; Published: July 24, 2024.
DOI: 10.15376/biores.19.3.6444-6458